Reducing Nonlinear Distortion in Optical Phase Conjugation using a Midway Phase-Shifting Filter

Monir Morshed, Arthur J. Lowery* and Liang B. Du

Center for Ultrahigh bandwidth Devices for Optical Systems (CUDOS),Department of Electrical & Computer Systems Engineering, Monash University, Clayton, VIC 3800, Australia

http://www.ecse.monash.edu.au

*arthur.lowery@eng.monash.edu.au

Abstract: The performance of optical phase conjugation (OPC) is improved by splitting the nonlinear element and inserting a phase-shifting filter. The maximum signal quality increases by 1.2 dB for 800-km 4-QAM 224-Gb/s CO-OFDM.

OCIS codes: (060.4510) Optical Communications ; (070.5040) Phase conjugation; (190.4380); Nonlinear optics,

1. Introduction

Fiber nonlinearity is the major limiting factor of transmission distance and spectral efficiency in long-haul high-bandwidth optical communication systems [1, 2]. Optical Phase Conjugation (OPC) [3] for mid-span spectral inversion (MSSI) is one method of mitigating the effects of fiber nonlinearity for multiple WDM channels [4, 5].

Recently, we proposed a method for improving the fundamental performance of third-order optical nonlinearity based OPC systems [6]. This method involved splitting the nonlinear element into two sections, suppressing the cross-phase modulation (XPM) products from the first element with a notch-filter before the second section, and then re-inserting the pump into the second section. Using numerical simulations, we showed that this method reduced the fundamental degradation introduced by OPC by 3 dB, giving an improvement in the maximum signal quality, Q_{max}, by 1 dB in a 10 × 80-km 4-QAM 224-Gb/s CO-OFDM system [6].

In this paper, we propose a method that gives a better performance improvement than the notch-filter OPC. This uses an in-line phase-shifting filter (PSF) between the two nonlinear sections of the OPC. Numerical simulations show that this phase-shifting filter OPC module has a 3.6 dB higher back-to-back signal quality, Q_{max} [7], compared with a conventional OPC module. This better back-to-back performance results in an improvement of the maximum Q_{max} by 1.2 dB in a 10 × 80-km 4-QAM 224-Gb/s CO-OFDM system.

2. OPC with phase-shifting filter

Figure 1(a) shows the details of the novel MSSI module using a two-part OPC with phase-shifting filter in between them. We found that the performance of the systems is optimum when the PSF also has a 6-dB loss in the phase-shifted region, shown by the purple line (▬).

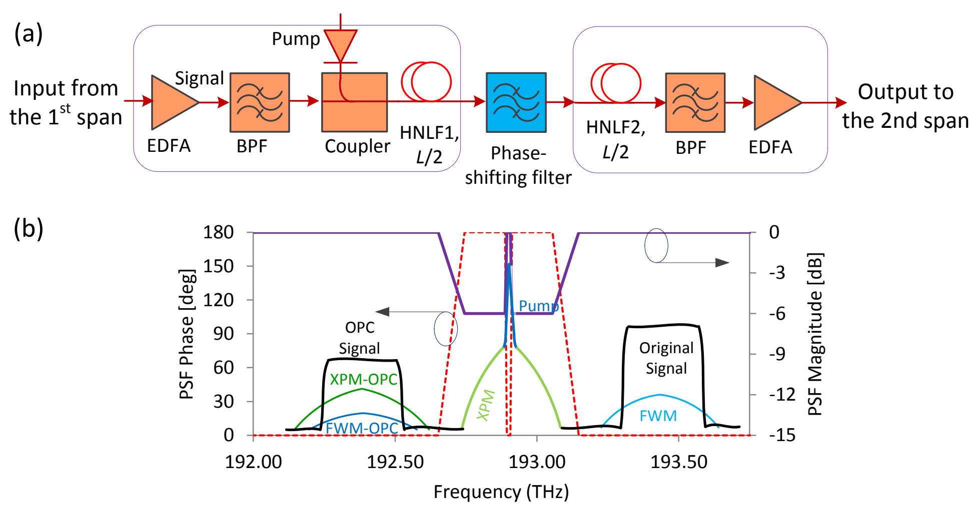

Fig. 1 (a): Block diagram of MSSI module; (b): spectra after the first half OPC and PSF characteristics.

The PSF has a frequency-dependent phase characteristic as shown by the gray dotted line (▪▪▪) in Fig. 1(b). This figure also shows representative spectra of: the original signal, pump, OPC signal, XPM distortions around the pump, four-wave mixing (FWM) distortions, XPM-OPC and FWM-OPC distortions [8]. XPM-OPC falls on the

OPC signal band and is the dominant degradation. Fortunately, the XPM-OPC distortion is generated in a two-stage process, via XPM. Thus, if we can suppress XPM, we can suppress XPM-OPC. To achieve this, the PSF's phase response must be zero for all the above spectral components except for the XPM distortions (▬) around the pump; the XPM products should be phase shifted by 180 degrees. Note that the phase of the pump is not shifted. After the PSF, all the spectral components shown in Fig. 1(b) are fed into the second highly nonlinear fiber (HNLF2), followed by a band-pass filter (BPF) and an output EDFA. Since the pump remains in phase with the input in the second part of the OPC module, HNLF2 generates OPC signals in phase with those generated by the first part.

We can explain the improvement in performance by considering the effect of the phase shift on the generation of XPM-OPC. Figure 2(a) illustrates the accumulated field of XPM products, E_{XPM} (▬), and its conjugate, $E_{XPM\text{-}OPC}$ (▬), along the HNLF when conventional OPC is used. E_{XPM} grows linearly along the fiber and $E_{XPM\text{-}OPC}$ grows quadratically [8]. Figure 2(b) shows the corresponding fields when a 180° phase shift is used in the PSF in the spectral range of XPM products. Applying this phase shift inverts the E_{XPM} vector. New contributions to E_{XPM} generated in HNLF2 are anti-phase with the E_{XPM} at the output of HNLF1; so the accumulated E_{XPM} reduces along HNLF2. As an additional benefit, the new $E_{XPM\text{-}OPC}$ field generated at any point in HNLF2 is anti- phase with the $E_{XPM\text{-}OPC}$ field at the output of HNLF1 due to the inverted E_{XPM} field. The accumulated $E_{XPM\text{-}OPC}$ field (▪▪▪) becomes zero at the end of the HNLF2. Thus, this PSF is expected to significantly improve system performance. Note, however, that we found that the filter should also have additional loss in the phase-shifted region for optimum cancellation, due to higher-order mixing processes.

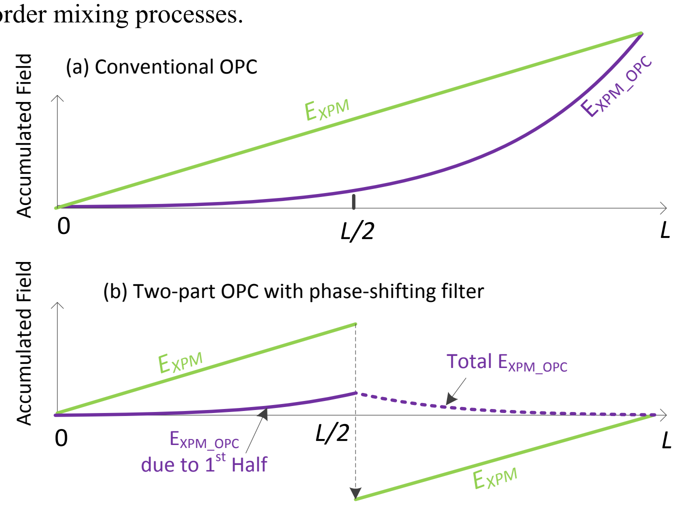

Fig. 2: One-stage (E_{XPM}) and two-stage ($E_{XPM\text{-}OPC}$) mixing of nonlinear products inside the OPC: (a) conventional OPC; (b) PSF OPC with PSF.

3. Simulation Results

We quantified the back-to-back performance of PSF OPC and also its performance in a CO-OFDM system (Fig. 3) using VPItransmissionMaker v8.7. The OFDM signal used a 1024-point inverse fast Fourier transform (IFFT); 920 subcarriers were modulated with 4-QAM and a 32-point cyclic prefix (CP) was inserted before each OFDM symbol. The total bit rate was 224-Gb/s, resulting in a net data rate of 200 Gb/s with 12% overhead for FEC and training. The optical link comprised 10×80-km spans of standard 0.2-dB.km^{-1} loss single mode fiber (S-SMF) with EDFAs to compensate the span losses. The OPC module is placed after the fifth span. A 60-km dispersion compensation fiber (DCF) was used just before the MSSI module [9]. The detail of the MSSI module is shown in Fig. 1(a). The nonlinear coefficient of the HNLF, γ is 11.5 W^{-1}.km^{-1}, its loss coefficient is 0.97 dB/km, and chromatic dispersion, CD is zero. The pump power into the HNLF is 10 dBm.

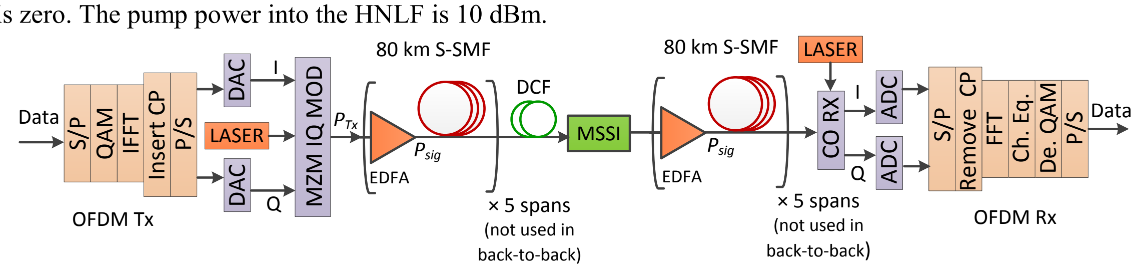

Fig. 3. Schematic of CO-OFDM transmission system. A detail of MSSI has been shown in Fig. 1(a).

Figure 4(a) shows the back-to-back Q versus input signal power into the HNLF. The blue curve with circles (●) shows the system performance with conventional OPC and the red curve with squares (■) shows the system performance with PSF OPC. The dotted purple line (▪▪▪) shows back-to-back performance when OPC is not used. The PSF improves the back-to-back signal quality, Q_{max}, by 3.6 dB at the optimum signal power.

Figure 4(b) shows the comparison of transmission performance between systems with conventional OPC (●) and phase-shifting filter OPC (■). The input power into the OPC module is the optimum power from the back-to-back simulations shown in Fig. 4(a), which are 2 dBm for conventional OPC system and 6 dBm for PSF OPC. The input power into the DCF was 4-dB less than the OPC input power. Results without OPC (▪▪▪) show the benefit of OPC. The system with conventional OPC shows 1-dB better Q_{max} than the system without OPC. The system with the phase-shifting filter has an additional 1.2-dB Q_{max} improvement at the optimal signal power.

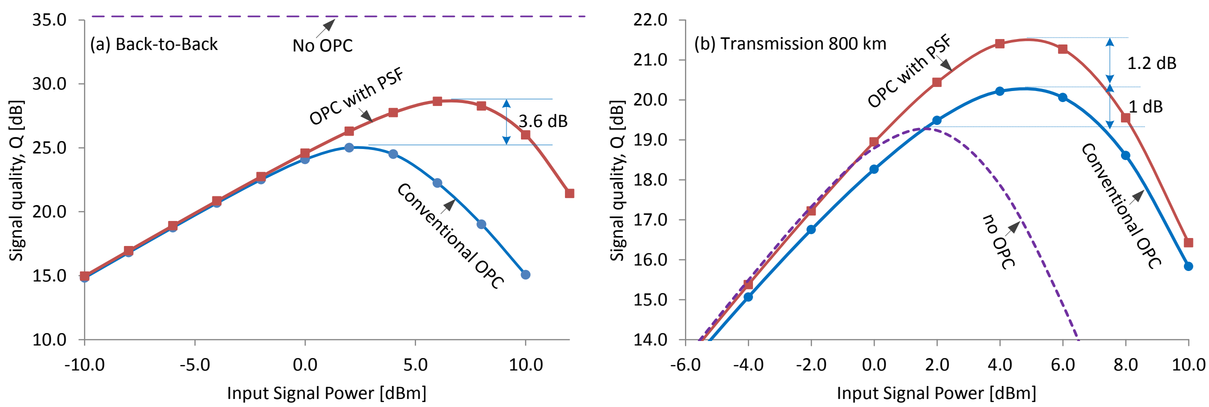

Fig. 4. Performance comparisons between the conventional OPC module and the two-part OPC module with PSF: (a) performance in back-to-back system; (b) performance in an 800-km transmission system.

4. Conclusion

We have proposed a new design of an OPC using third-order nonlinearity to improve the back-to-back performance of CO-OFDM systems using MSSI. Our proposed design improves the back-to-back performance by 3.6 dB and the transmission performance at optimum power by 1.2 dB in a 10 × 80-km 4-QAM 224-Gb/s CO-OFDM system. PSF OPC gives a better improvement than two-stage OPC with a phase-flat notch-filter [6].

Acknowledgement

This research was conducted by the Australian Research Council Centre of Excellence for Ultrahigh bandwidth Devices for Optical Systems, CUDOS (Project number CE110001018). We should like to thank VPIphotonics.com for the use of VPItransmissionMaker.

Reference

1. A. D. Ellis, Z. Jian, and D. Cotter, "Approaching the non-linear Shannon limit," J. Lightwave Technol. **28**, 423-433 (2010).
2. R.-J. Essiambre, "Exploring capacity limits of fibre-optic communication systems," in *34th European Conference on Optical Communication, ECOC 2008*(2008).
3. A. Yariv, D. Fekete, and D. M. Pepper, "Compensation for channel dispersion by nonlinear optical phase conjugation," Opt. Lett. **4**, 52-54 (1979).
4. S. L. Jansen, S. Spalter, G. D. Khoe, H. de Waardt, H. E. Escobar, L. Marshall, and M. Sher, "16×40 gb/s over 800 km of SSMF using mid-link spectral inversion," IEEE Photon. Technol. Lett. **16**, 1763-1765 (2004).
5. L. B. Du, M. M. Morshed, and A. J. Lowery, "Fiber nonlinearity compensation for OFDM super-channels using optical phase conjugation," Opt. Express **20**, 19921-19927 (2012).
6. M. Morshed, A. J. Lowery, and L. B. Du, "Improving performance of optical phase conjugation by splitting the nonlinear element," Opt. Express **21**, 4567-4577 (2013).
7. A. J. Lowery, S. Wang, and M. Premaratne, "Calculation of power limit due to fiber nonlinearity in optical OFDM systems," Opt. Express **15**, 13282-13287 (2007).
8. M. Morshed, L. B. Du, and A. J. Lowery, "Mid-Span Spectral Inversion for Coherent Optical OFDM Systems: Fundamental Limits to Performance," J. Lightwave Technol. **31**, 58-66 (2013).
9. P. Minzioni, F. Alberti, and A. Schiffini, "Optimized link design for nonlinearity cancellation by optical phase conjugation," IEEE Photonics Technology Letters **16**, 813-815 (2004).